Human activity monitoring system with commodity WiFi infrastructure using channel state information

Hicham Boudlal[1], Mohammed Serrhini[2], Ahmed Tahiri[1]
[1]Laboratory of ACSA, Faculty of Sciences, Mohammed First University, Oujda, Morocco
[2]Laboratory of LaRI, Faculty of Sciences, Mohammed First University, Oujda, Morocco

Article Info	ABSTRACT
	Human activity detection is a research field that has been growing rapidly for the last few decades. It opens a wide field of applications in the fields of healthcare, smart homes, robotics, human-media interaction, surveillance and security. WiFi-based solutions have received a lot of attention lately. These are based on the idea that nearby wireless signals are affected by human bodies. Reflections are produced by the presence of static objects like walls and furniture, while additional propagation paths are produced by the presence of dynamic objects such humans. This paper proposes using WiFi for a low-cost, device-free human activity monitoring system, as it is readily available in the office and home these days. It is also ubiquitous in nature as it collects information about the environment while providing Internet. The idea behind this approach is to acquire and model changes in multipath WiFi radio waves due to human movement. Experimental validation in practical situations with varying occupants, different environmental conditions, and interference from WiFi devices is used to demonstrate robustness and scalability. *This is an open access article under the [CC BY-SA](#) license.*

Corresponding Author:

Hicham Boudlal
Laboratory of ACSA, Faculty of Sciences, Mohammed First University
BV Mohamed VI BP 717 60000 Oujda, Morocco
Email: hicham.boudlal5@gmail.com

1. INTRODUCTION

Human activity recognition and monitoring have received considerable interest recently because of numerous applications to monitor human activity and behavior within indoor spaces. These applications include health monitoring, fall detection for the elderly, activity detection for smart home energy efficiency, and several more internet of things (IoT)-based applications [1], [2]. Traditionally, wearable technology or technologies like depth and infrared cameras have been used to recognize and monitor activities. These systems have non-negligible deployment costs and high overhead. The camera-based approach primarily makes use of computer vision processing technology, which is restricted by line of sight and light intensity, necessitates rigorous climatic conditions, and poses the danger of leaking personal information. The wearable device-based approach may produce excellent accuracy, but because it must be fastened to the user's hand or body, there could occasionally be discomfort and higher additional costs [3], [4].

WiFi has recently been the focus of a lot of research on activity monitoring due to its widespread availability in indoor spaces, making the deployment of additional infrastructure unnecessary, which is an advantage over the current activity monitoring approach. These systems include an access point (AP) and one or more WiFi enabled devices dispersed throughout the environment. As a person is engaged in some activity, body movement impacts wireless signals as well as changes the multipath profile of the system [5]-[7]. WiFi signal is affected by reflection, diffraction and scattering caused by objects or people in a room as it travels

from the transmitter to the receiver. Human activities affect the amplitude and phase of the signal, which is reflected in the phase and amplitude of the received signal. The phase and amplitude of WiFi signals can therefore be used to determine a person's activity. WiFi signals can be used for activity recognition since the channel state information (CSI) gives the phase and amplitude of each subcarrier for each pair of receiver and transmitter antennas. Because it provides more accurate channel information than, for example, the received signal strength indicator (RSSI), CSI is one of the most commonly used units of measurement for this purpose of activity monitoring [8], [9].

In light of this, in this paper we present a non-intrusive and reliable human activity monitoring system that uses low-cost WiFi devices widely available in the home and doesn't necessitate subjects wearing or carrying any equipment. These are the main contributions of this work:

- We are exploiting the possibility of using WiFi signals to monitor human activity without a device using passive Wi-Fi sensing with a low-cost commercial Wi-Fi card (Intel 5300).
- The design of a unique WiFi-based system for monitoring human activity is proposed.
- A thorough examination of the characteristics of the CSI change brought on by human presence.
- The proposed approach is implemented as a prototype system.
- Experiments are conducted for validating performance of proposed approach in different environments and in line-of-sight (LOS) and non-LOS (NLOS) conditions.

The structure of this paper is outlined as shown in: section 2 provides some background information, followed by the details of the technology. In section 3, we present the design details and an overview of the system architecture. Section 4 describes the experimental environment, hardware/software configuration, implementation, and evaluation. Finally, section 5 presents conclusions and future research directions.

2. BACKGROUND

In this section, we first describe the WiFi signal attributes for extracting human motion information. Two attributes are explained below, RSSI and CSI. Then, we highlight a comparison between these concepts.

2.1. Received signal strength indication

RSSI is used internally in the IEEE 802.11 standard to represent connection quality. RSSI is a device-related approach that employs signal strength determined under the direct effect of multipath shading and fading [10]. WiFi devices are capable of receiving signals that reflect the path loss of wireless signals over a specific distance. The log-normal distance path loss (LDPL) model is often employed to quantify this reflection and estimate the path loss of the wireless signal [11], [12]:

$$P(d) = P(d_0) + 10\gamma log \frac{d}{d_0} + X_\delta \tag{1}$$

$P(d)$ is the RSSI measurement, which indicates the path loss at distance in decibels (dB). $P(d_0)$ is the path loss at the reference distance d_0, γ is the path loss's exponent, and X_δ is flat fading's zero average normal noise.

Due to its native implementation in the medium access control (MAC) layer of every given wireless device for quality of service evaluation, RSSI is widely used in indoor location systems. RSSI is a technique that uses radio frequency detection devices and utilizes the signal strength provided by shadowing and multipath fading. If there's a human between the wireless connections, this will reduce the strength of the WiFi signal, therefore the difference between the strength of the broadcast and received signal could be measured. But this metric necessitates that multiple anchor stations have a unique location estimate and it suffers from multipath and shadowing effects. While the RSSI is a widely used and easily obtainable metric in WiFi devices, it can be difficult to capture real-time signal fluctuations using this approach. Furthermore, several studies have shown that RSSI may not always provide accurate and reliable information in many application contexts, including even static indoor environments. As a result, the stability of RSSI as a metric remains uncertain and unreliable, despite its basic and simple nature that does not require additional hardware [12].

2.2. Channel state information

CSI describes the properties of the channel used by the sender and receiver, reflecting the scattering and refraction that occur during transmission, as well as representing the attenuation of the wireless signal as it propagates between the sender and receiver. The IEEE 802.1n Wi-Fi standard utilized in this research supports multiple input and multiple output (MIMO) to transmit signals between transmitters and receivers. WiFi standards utilize orthogonal frequency division multiplexing (OFDM) communication [13], [14] that transmits multiple signals in parallel on different frequencies in the bandwidth to achieve this. OFDM separates

the channel into various subcarriers and sends the data on the subcarriers using the same modulation and coding scheme. Due to the channel's division into subcarriers, OFDM can manage frequency selective fading brought on by multipath. Each subcarrier faces an independent flat fading since it is small in comparison to the coherence bandwidth. In this way, multipath effect on different subcarriers could be regarded as more or less uncorrelated. Each of these subcarriers can be characterized by using the CSI [15], [16].

For OFDM subcarriers, the signal strength and phase information are represented by the CSI information. The signal received could be represented as (2).

$$y = H \times x + n \tag{2}$$

The received signal y is related to the transmitted signal x by the channel noise n and the channel frequency response (CFR) represented by a complex-valued matrix H. The CSI matrix H is defined as an $m \times n \times w$ matrix, where m denotes the number of transmitter antennas, n denotes the number of reception antennas, and w denotes the number of subcarriers, for each specific subcarrier within each spatial stream. This matrix provides detailed information on the channel's temporal and spectral characteristics and captures any changes caused by a multipath effect at small scales. To represent the CSI components H of every received packet in a MIMO system with m transmitters and n receivers, we can use (3).

$$H = \begin{bmatrix} H_{1,1} & \cdots & H_{1,n} \\ \vdots & \ddots & \vdots \\ H_{m,1} & \cdots & H_{m,n} \end{bmatrix} \tag{3}$$

Each element $h_{i,j} = (h_1, h_2, \ldots, h_w)$ of the matrix is a vector containing the channel state h_k for each k-th subcarrier for every transmitting (i) and receiving (j) antenna pair. The value h_k provides information on the amplitude and phase of the corresponding subcarrier and could be expressed as follows, where $[h_k]$ represents the amplitude and θ represents the phase [17].

$$h_k = [h_k]e^{j sin\theta} \tag{4}$$

The transmitter sends long learning symbols (LTS), that include predetermined information about each subcarrier in the packet preamble, to measure the CSI. In situations where LTS are received, the WiFi receiver calculates the CSI using the received signal and the original LTS. But multi-channel, receiver/transmitter processing, hardware as well as software errors, and other issues all have an influence on the CSI in real-world systems [8]. Figure 1 show the multipath effect of WiFi signals propagation.
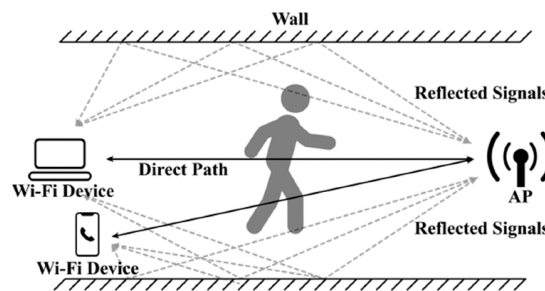

Figure 1. Multipath effect of WiFi signals propagation

Wireless transmission systems are susceptible to the multipath phenomenon, which occurs when transmitted signals do not reach the receiving antenna directly. This phenomenon arises from various external elements that affect the propagation of the signal, resulting in a combination of reflections, scattering, and attenuation. Reflection refers to the phase change that occurs when the signal bounces off a surface, which can result in constructive or destructive interference. Scattering occurs when the signal encounters objects or irregularities in the path, causing it to spread out and change in shape. Attenuation refers to the loss of signal strength as it travels through the medium, which can occur due to factors such as absorption, diffraction, or interference.

The static objects in the environment will affect the multipath consistently, while dynamic objects like human body will affect it variably. This multipath variation is due to human activity. This could be passive

movement such as breathing or active movement such as walking [18]. Based on the amplitude and phase of the received signal, we can determine if the signal was modified by human activity between transmission and reception and extract the type of activity the person was performing. The focus of this paper will be on the use of amplitude.

2.3. RSSI compared to CSI

With OFDM systems, each subcarrier is faced with a narrowband fading channel, and acquiring CSI at every subcarrier will result a diversity in the dynamics of the observed channels. These are the main advantages of using CSI over RSSI, which averages changes over the entire WiFi bandwidth and thus is unable to capture changes in certain frequencies [19]. Table 1 shows the differences of RSSI and CSI.

Table 1. The difference among CSI and RSSI [20]

Category	RSSI	CSI
Resolution of time	Packet	Cluster of multipath signals
Resolution of frequency	None	Subcarrier
Stability	Low	High
Dimension	One dimension	High dimension
Universality	All WiFi devices	Some WiFi devices

3. SYSTEM DESIGN

In this section, we aim to provide a comprehensive understanding of our system design. Firstly, we will provide an overview of the entire system, highlighting its key features and functions. We will then delve into each individual component, detailing their specific roles and interactions.

3.1. System overview

Our system is designed to detect movement using variations in the correlation between CSI sequence frames that are sensitive to human movement. By identifying periods of greater fluctuation, we can determine whether the subject's movements have affected the radio frequency (RF) environment, and thus detect movement. As shown in Figure 2, the system consists of three main components. The CSI data is collected using dedicated hardware and can be transmitted to the system either in batches or in real-time through a buffer. The collected data is then pre-processed to eliminate errors and reduce noise. Finally, the pre-processed data is analyzed to identify any periods of greater fluctuation in the correlation between CSI sequence frames, which can indicate movement.
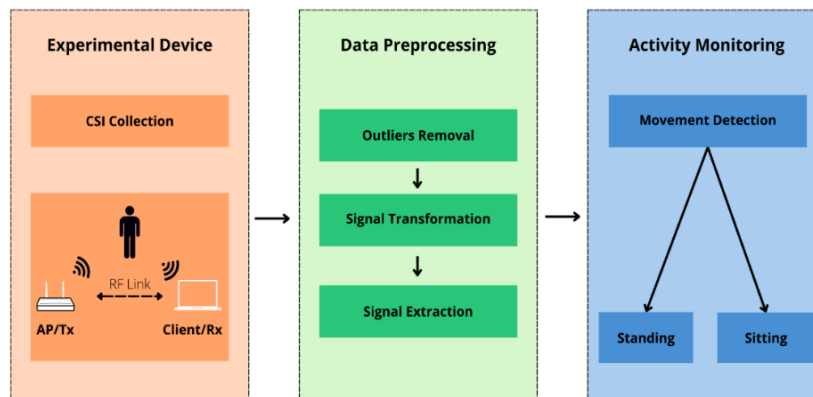

Figure 2. Overall system diagram

3.2. CSI collection
3.2.1. Device architecture

According to (2), to estimate the CSI, a transmitter (Tx) must send a pilot signal to a receiver (Rx), and the CSI must then be calculated. The receiver estimates CSI using a signal which is often a ping packet that is sent from Tx to Rx. The Linux 802.11n CSI tool based on the Intel 5300 network interface card (NIC) is a tool available for this collecting [21]. Figure 3 illustrates the configuration of the device used to collect data.
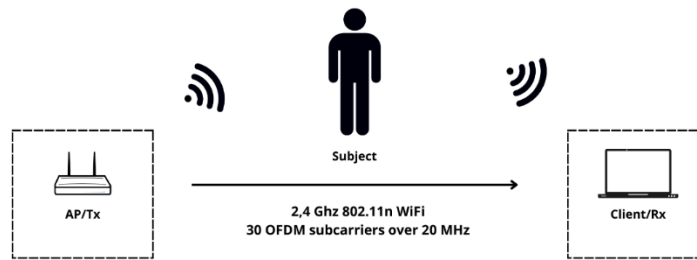
Figure 3. CSI collection illustration

In this architecture, Tx and Rx have dedicated continuous transmission, and Rx will estimate CSI over incoming packets. This reduces hardware, computational as well as power costs. In COVID 19 pandemic context, a low installation cost solution is desired.

3.2.2. Comparison of the LOS and NLOS modes

In order to compare the system's performance under different human positions, we studied two modes of operation: LOS and NLOS [22]. Figure 4 shows the illustrations of the two modes, with Figure 4(a) depicting the LOS mode and Figure 4(b) depicting the NLOS mode. In the LOS mode, the person is positioned in a straight line between the Tx and the Rx, as illustrated in Figure 4(a). On the other hand, in the NLOS mode, the person is not on a straight line but rather somewhere between Tx and Rx. The predicted distance between the person's body and the line that connects the antenna and the receiver is 1 m, as illustrated in Figure 4(b).
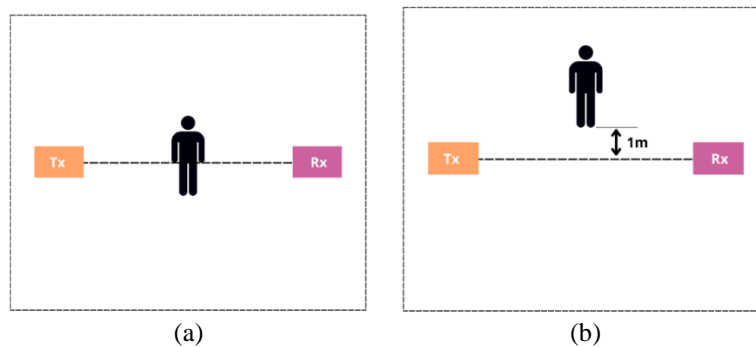

(a)   (b)

Figure 4. Illustration of LOS and NLOS mode (a) light of sight and (b) non light of sight

3.3. Data preprocessing

WiFi CSI data often contains a significant amount of noise, even with high-quality hardware and optimal configuration settings. This noise can be attributed to various factors, such as the presence of surrounding and reflected radio waves, as well as potential hardware and software issues. Therefore, data preprocessing plays a critical role in developing a dependable and precise human activity detection model using WiFi CSI data. By properly processing the data, it becomes possible to create a reliable and accurate model.

3.3.1. Outliers' removal technique

CSI can be sensitive to environmental changes, leading to undesirable noise that makes detecting small activities challenging. To mitigate this issue, we employ various filters to the CSI data. A low pass filter [23] is initially used to remove high frequency signal elements. However, internal changes of state, such as transmission power, rate adaptations, and thermal noise in devices, may still produce noise in the CSI's amplitudes and phases. To address this, we utilize the Hampel filter [24]. Furthermore, we apply a moving average filter [23], which is a running mean filter, to further reduce high frequency noise. The efficacy of these filters is demonstrated in Figure 5, which is divided into four sub-figures. Figure 5(a) shows the original CSI signal, which is affected by high frequency noise. Figures 5(b), 5(c), and 5(d) depict the CSI amplitude after applying the low pass filter, Hampel filter, and running mean filter, respectively. As shown in these sub-figures, the filters successfully reduce the noise and improve the quality of the CSI signal.

(a)   (b)

(c)   (d)
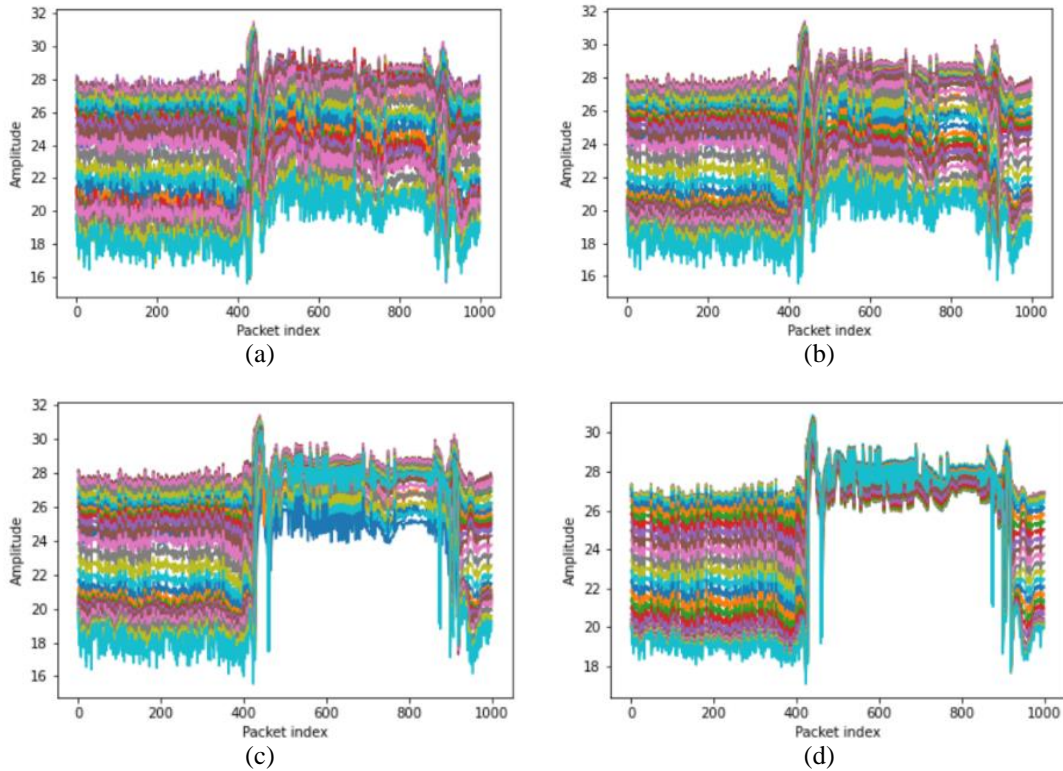
Figure 5. Illustrates a comparison of the amplitude of CSI before and after filtering, highlighting the resulting outcomes (a) original signal, (b) lowpass filter to isolate frequencies bellow 10 Hz (order=5), (c) hampel filter to reduce high frequencies moise (window size=10, significance=3), and (d) running mean filter for smoothing (window size=10)

3.3.2. Signal transformation using on short time fourier transform

We perform time-frequency analysis on a time series of CSI measurements using signal transform algorithms. To individually compute the fast fourier transform (FFT) coefficients on each segment, we employ the short-time fourier transform (STFT) method. This involves separating the input into shorter segments of equal length, as shown in (5). The STFT enables us to determine how the dominant frequencies change over time by representing the time series data in both the time and frequency domains [8]. Figure 6 illustrates the STFT.

$$X(t,k) = \sum_{n=-\infty}^{\infty} x[n]w[n-t]e^{-jkn} \tag{5}$$

Where t is time index, k is frequency index and w is window function.
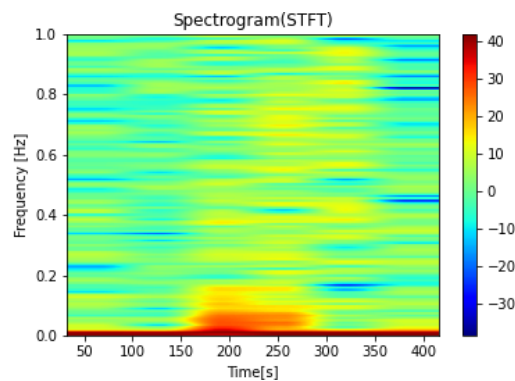

Figure 6. Illustrates the STFT

3.3.3. Signal extraction via principal component analysis

Signal extraction techniques are used to retrieve signal targets from raw or preprocessed measurements of CSI, but processing these measurements can be computationally intensive. To mitigate this issue, principal component analysis (PCA) is commonly employed for blind signal separation and feature extraction. By using an orthogonal transformation technique, the input matrix is transformed into a set of principal components. Despite the input variables being correlated, the resulting principal components are linearly uncorrelated [8]. Figure 7 demonstrates the application of PCA to reduce the dimensionality of CSI data.
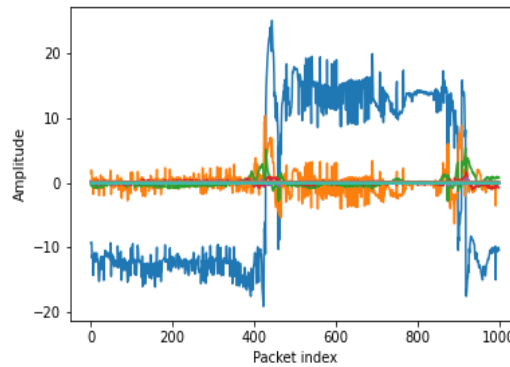
Figure 7. Illustrates the PCA for reducing the dimensions of CSI data

4.   EXPERIMENT AND ANALYSIS

In this section, we provide a comprehensive description of the environment used for our experiment. This includes details of the hardware and software configuration, as well as relevant settings and parameters. Additionally, we present the experimental results obtained from our approach and provide a detailed performance evaluation of its effectiveness.

4.1. Experimental environment

The dimensions and parameters of the two different environments where the experiments were conducted are displayed in the Table 2. Two devices were used as a Tx and a Rx to set up instrumentation in two different test environments. The Tx and Rx devices represented the AP transmitter and the receiver laptop, respectively. Both devices were positioned at 0.75 m above the ground to ensure an unobstructed signal path. The physical environment of the laboratory and office remained unchanged during the experiment, and both environments were equipped with tables, desks, computers, and various pieces of wood or metal equipment. The experimenter's position and direction were constant in both test scenarios during data collection and estimation. Figure 8 illustrates the two experimental environments, with Figure 8(a) depicting the laboratory and Figure 8(b) depicting the office.

Table 2. Summary of experiment parameters

Characteristics and parameters	Environment	
	Laboratory	Office
Dimensions	8m * 9m	4m * 9m
Occupancy	1 Person	1 Person
Bandwidth	20MHz	20MHz
Channel	11 (2462MHz)	11 (2462MHz)
Frequency	2.417GHz	2.417GHz
Antennas	3Rx * 2Tx	3Rx * 2Tx
Subcarriers	30	30

4.2. Experimental setting

We conducted an experiment in a Wi-Fi network 802.11n at 2.4 GHz using a single off the shelf Wi-Fi device (i.e., HP 290 G1 MT business computer) connecting with a commercial wireless AP (i.e., TP-LINK TD -W8961N) which acts as a double antenna transmitter. The laptops run Ubuntu 14.0.4.4 LTS with the 4.2.0-27 kernel and are equipped with an Intel WiFi Link 5300 card with 3 antennas that act as a receiver. On the same laptop, MATLAB is installed to process the offline data collection and provide information about

human activity. Most of the interesting activities occur within a few seconds. For capturing the signal impacted by these short-term activity, the laptop communicates with the WiFi access point by sending ICMP echo request packets every 10 ms and receiving ICMP echo reply packets, the sampling rate is 100 Hz. We extract CSI data from the received packets for 30 subcarrier groups of 20 MHz channel bandwidth using a modified version of an open source wireless driver [21]. Table 3 provides a list of the hardware and software utilized for the experience.

(a)   (b)
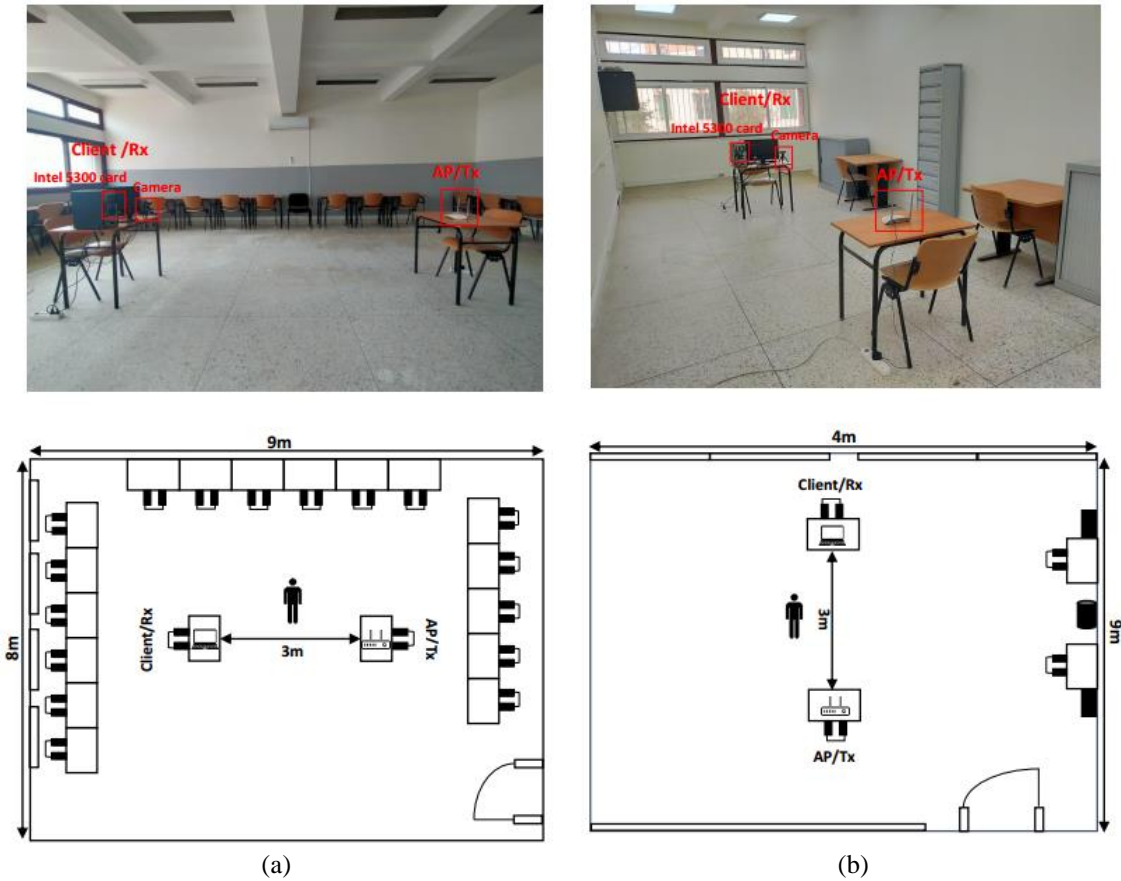
Figure 8. Experimental environments (a) the laboratory and (b) the office

Table 3. Lists of experimental hardware and software

Device name	Role	Hardware/Software	Specification and use
Laptop	Rx	HP 290 G1 MT Business PC	Receiving WiFi packets
Access Point	Tx	TP-LINK TD-W8961N	Transmitting WiFi packets
Network interface Card	Intel 5300	Intel 5300 Mini Wireless Network Card, 450Mbps, 3 antennas 6dbi, INTEL5300AGN	Receive CSI data
Software	MATLAB platform	MATLAB R2018b	Constructing system
Camera	Take pictures automatically	EKACOM Webcam 1080P with Microphone, Full HD	Capturing activity to validate the accuracy of the system's results

4.3. Experimental results

We conducted real experiments in a laboratory and office environment, the furnishings and placement of AP transmitter and receiving laptop are illustrated in Figure 8, as well as distance between the transmitter and receiver which is 3 m. In each scenario (LOS and NLOS) as shown in Figure 4 of each environment, a volunteer continuously performs the sitting and standing activities. While the volunteer was performing the activities, a stable WiFi signal between the router and receivers would ensure that the CSI was collected and stored for future reference. Figure 9 shows the operating interface of the transmitter and receiver, with Figure 9(a) representing the transmitter interface and Figure 9(b) representing the receiver interface. There is a total of 1000 packets sent on the transmitter.

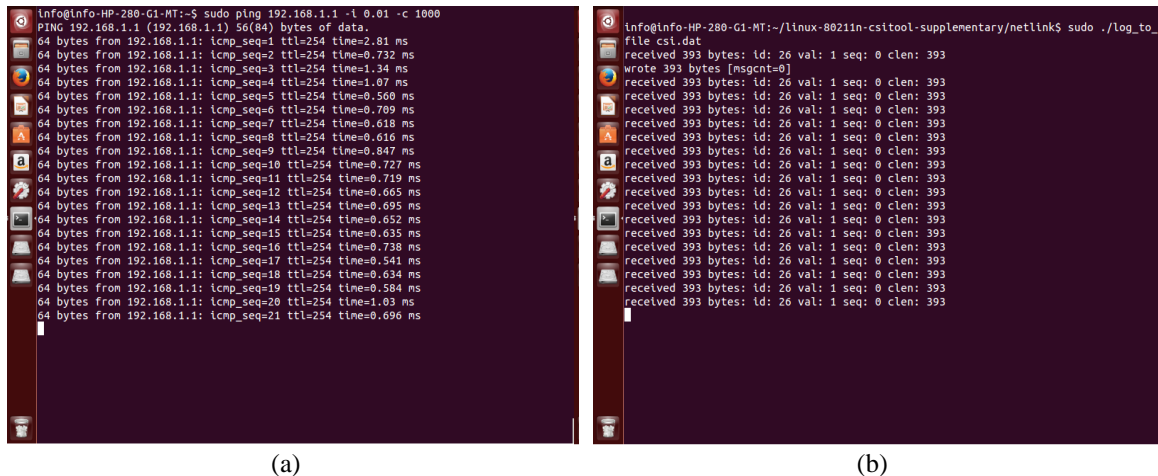(a)   (b)

Figure 9. Shows operating interface of the transmitter and receiver (a) transmitter interface and (b) receiver interface

To investigate the CSI data collected during our experiments, we analyzed packets that had a fixed size of 393 bytes. After being traced, the CSI data was stored in a .dat file. The receiver laptop played a crucial role in the process by receiving and logging the signal. We then explored the data provided by the CSI packets to gain insights into the performance of our system. Figure 10 illustrates an example of a CSI packet for reference.
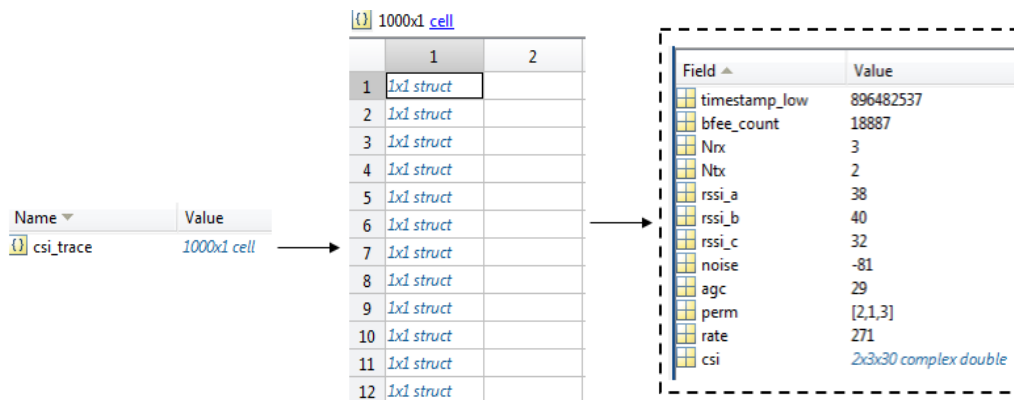
Figure 10. A sample CSI packet

We tested various activities in both lab and office environments to see whether they had different CSI change patterns in both LOS and NLOS locations. Since the environments were small, we limited the set of test activities to sitting and standing. These activities were selected for their ease of reproducibility and representativeness of realistic home behavior. In Figure 11, we illustrate how human movement induces large and rapid changes in the CSI of 30 subcarriers and all antennas, relative to a person sitting and standing between a WiFi transmitter and receiver. Figure 11 consists of four sub-figures, which show CSI amplitude heatmap plots for the LOS and NLOS environments in the laboratory (Figure 11(a) and Figure 11(b)), and for the office environment (Figure 11(c) and Figure 11(d)).

However, with the numerical graph, the shape is clearer, as illustrated in Figures 12. Figure 12 shows the amplitude of the CSI of 30 subcarriers and all antennas for the same LOS and NLOS environments in the laboratory (Figure 12(a) and Figure 12(b)), and for the office environment (Figure 12(c) and Figure 12(d)). During the first 400 packets, the person remains stationary before starting to stand or sit. The amplitudes of the CSIs for all antennas are relatively stable when the person is not moving, but they shift drastically once activity starts. This observation strongly implies that fine-grained surveillance of human activities can be performed without a device by utilizing the CSI from commonly available WiFi devices.
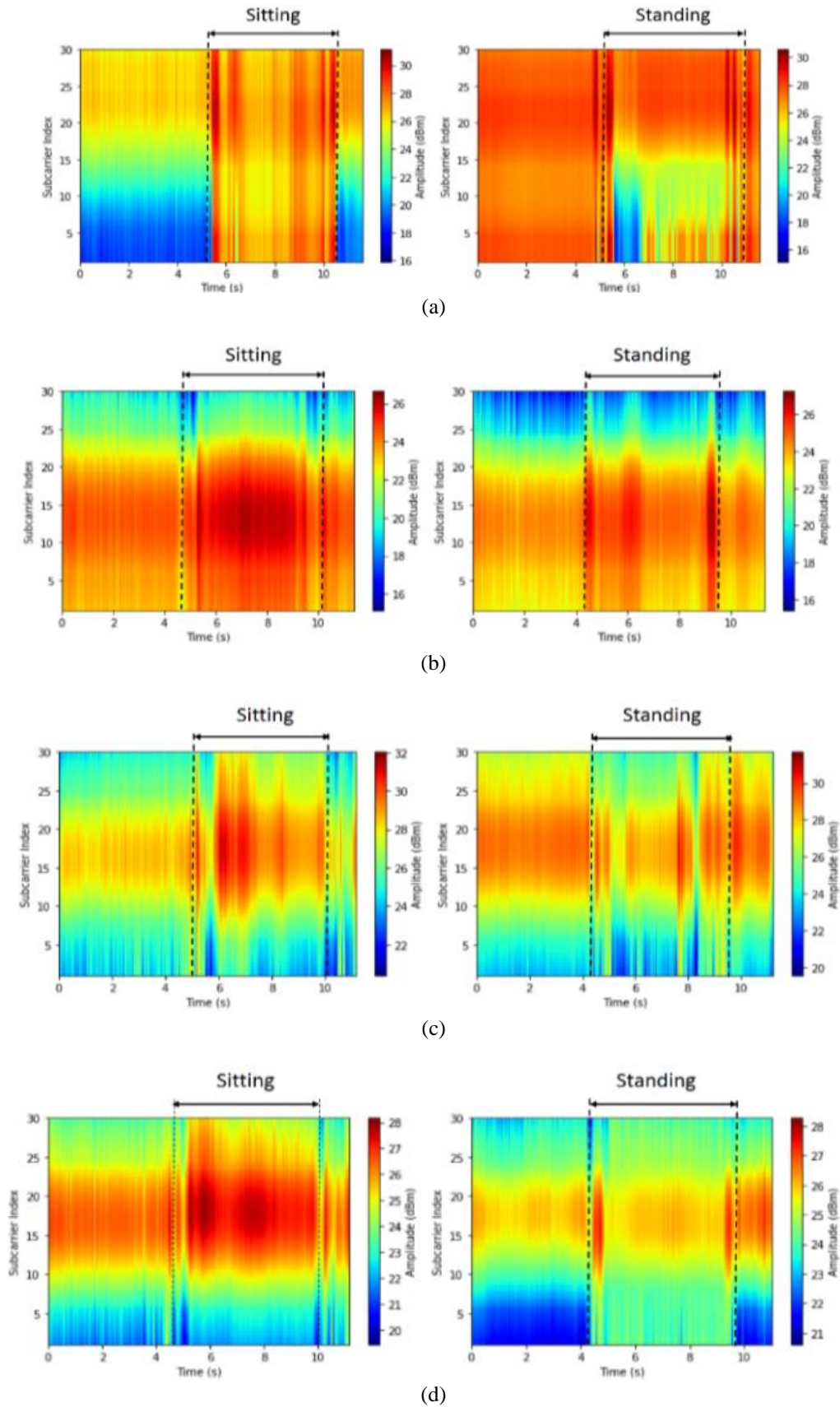
Figure 11. Shows CSI amplitude heatmap plot sitting and standing activity in (a) LOS at Laboratory, (b) NLOS at Laboratory, (c) LOS at office, and (d) NLOS at office
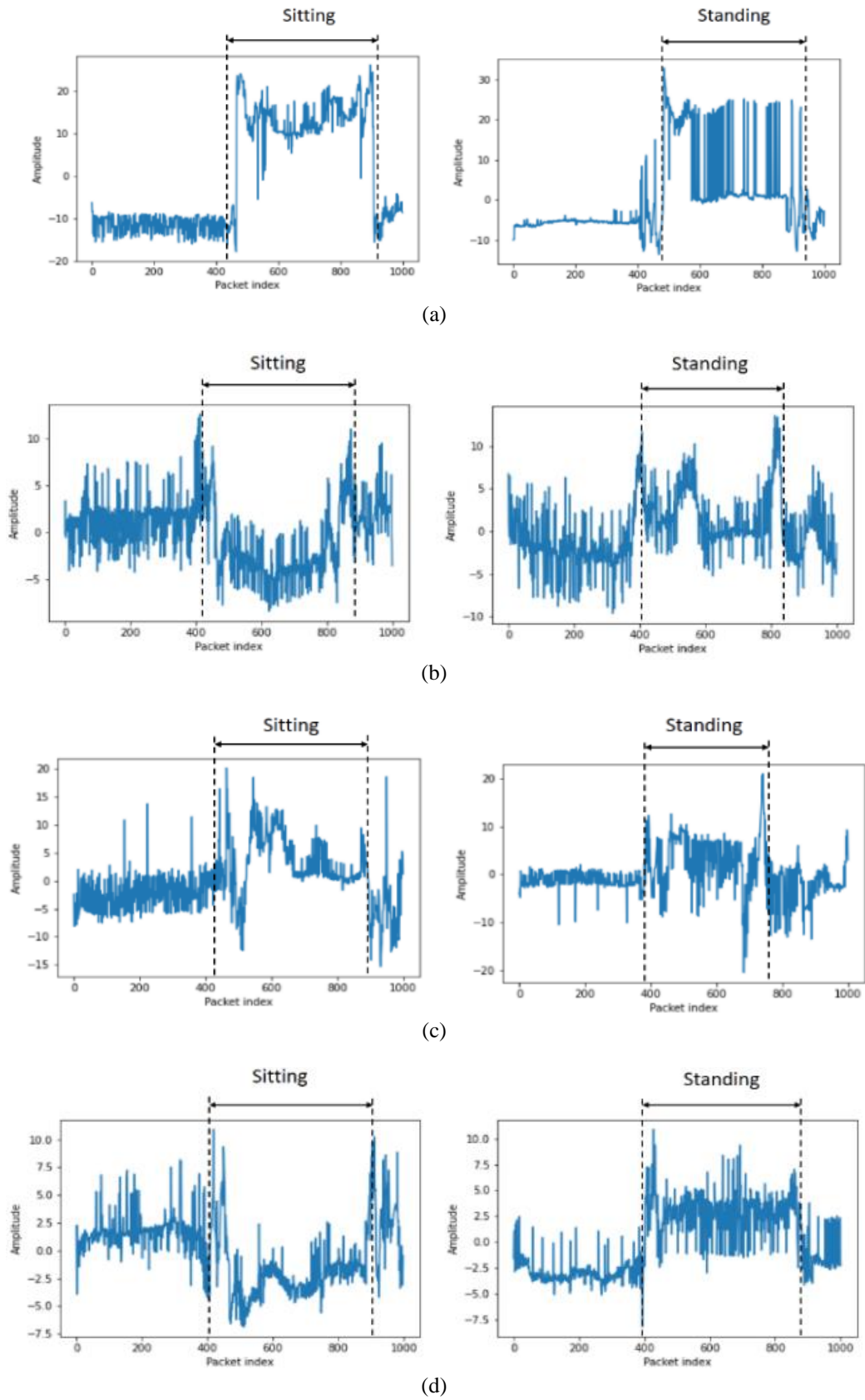
Figure 12. Shows CSI amplitude of 30 subcarriers and all antennas (a) LOS at Laboratory, (b) NLOS at Laboratory, (c) LOS at office, and (d) NLOS at office

To validate our proposed system, we deployed a camera to record the activities [25]. Obviously, achieving high accuracy in activity recognition means good performance of the recognition system. In Figure 13, we present the results of our analysis, which consists of four sub-figures labeled (a) through (d). Figure 13(a) shows the first PCA for all antenna on 30 subcarriers, while Figure 13(b) shows the processing data in MATLAB. Figure 13(c) shows the current CSI package ID attached to the photo, and Figure 13(d) shows the photo taken by the camera of each frame. These results demonstrate that we can accurately monitor human activity. Our model analysis and these results are in accordance.
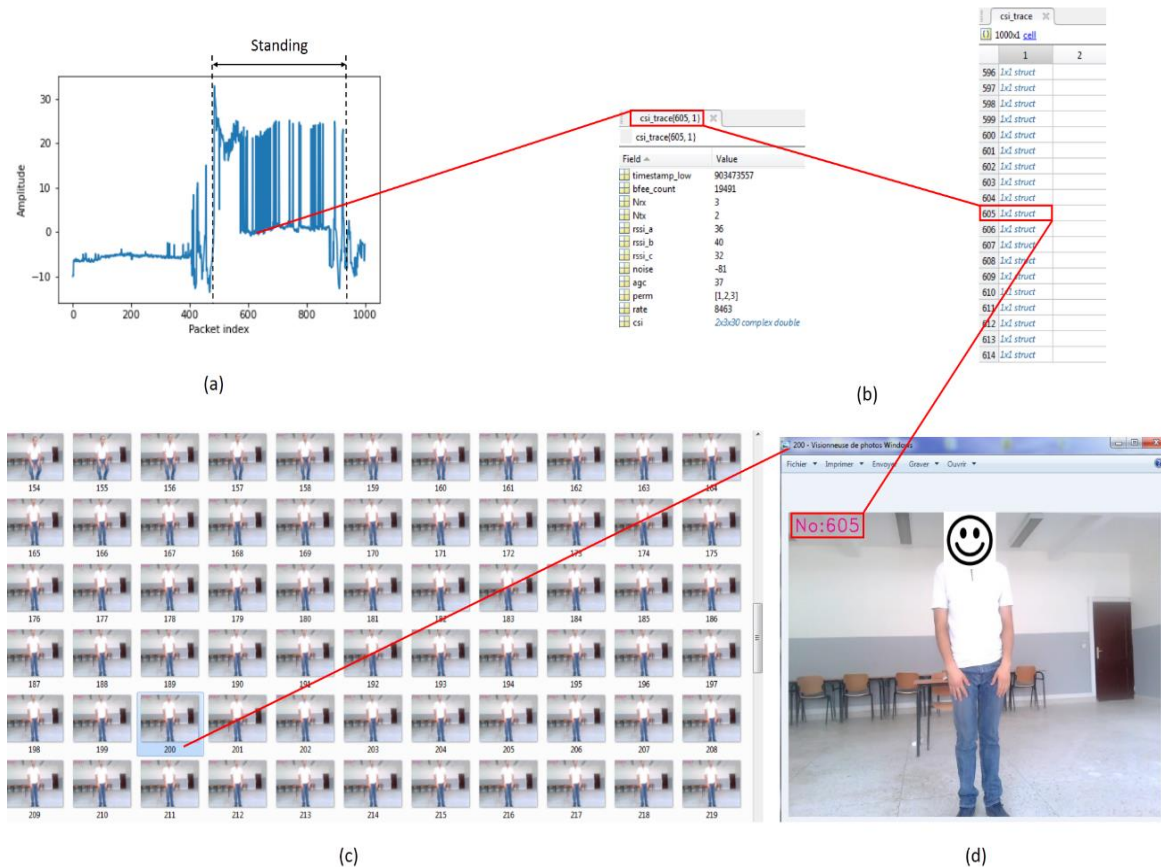
Figure 13. shows the current CSI package ID attached to the photo taken by the camera (a) the first PCA for all antenna on 30 subcarriers, (b) processing data in MATLAB, (c) current CSI package ID attached to the photo, and (d) photo taken by the camera of each frame

5. CONCLUSION

WiFi-based human activity monitoring can be used in a variety of applications that focus on humans and can herald a new era of non-contact sensing. These human activity monitoring systems do not require additional hardware as the majority of homes today already have WiFi enabled hardware. Unlike wearable human activity monitoring technology, it does not require the user to wear or carry a device. In addition to solving the limitations of vision-based human activity monitoring systems, it also preserves privacy, does not require line of sight, and can pass through walls. In this paper, we design and implement a low-cost, non-intrusive human activity monitoring system exploiting the amplitude of channel state information available in commodity WiFi devices. Extensive experiments conducted both in the laboratory and in the office demonstrate how our proposed approach utilizing existing WiFi network can reach equivalent or better accuracy than the current sensor-based approach. Future work will address numerous challenges, such as how to use the CSI phase data, how to make the system reliable in various dynamic environments, and how to keep track of the activities of several users.

REFERENCES

[1]   Z. Wang *et al.*, "A survey on human behavior recognition using channel state information," *IEEE Access*, vol. 7, pp. 155986–156024, 2019, doi: 10.1109/ACCESS.2019.2949123.
[2]   B. Fu, N. Damer, F. Kirchbuchner, and A. Kuijper, "Sensing technology for human activity recognition: A comprehensive survey," *IEEE Access*, vol. 8, pp. 83791–83820, 2020, doi: 10.1109/ACCESS.2020.2991891.
[3]   T. Li, C. Shi, P. Li, and P. Chen, "A novel gesture recognition system based on CSI extracted from a smartphone with nexmon firmware," *Sensors (Switzerland)*, vol. 21, no. 1, pp. 1–19, Dec. 2021, doi: 10.3390/s21010222.
[4]   A. Uchiyama, S. Saruwatari, T. Maekawa, K. Ohara, and T. Higashino, "Context recognition by wireless sensing: A comprehensive survey," *Journal of Information Processing*, vol. 29, pp. 46–57, 2021, doi: 10.2197/ipsjjip.29.46.
[5]   M. A. A. Al-qaness, "Device-free human micro-activity recognition method using WiFi signals," *Geo-Spatial Information Science*, vol. 22, no. 2, pp. 128–137, Apr. 2019, doi: 10.1080/10095020.2019.1612600.
[6]   W. Li, R. J. Piechocki, K. Woodbridge, and K. Chetty, "Physical activity sensing via stand-alone wifi device," in *2019 IEEE Global Communications Conference, GLOBECOM 2019 - Proceedings*, Dec. 2019, pp. 1–6, doi: 10.1109/GLOBECOM38437.2019.9013750.
[7]   Y. Ge *et al.*, "Contactless WiFi sensing and monitoring for future healthcare - emerging trends, challenges, and opportunities," *IEEE Reviews in Biomedical Engineering*, vol. 16, pp. 171–191, 2023, doi: 10.1109/RBME.2022.3156810.
[8]   Y. Ma, G. Zhou, and S. Wang, "WiFi sensing with channel state information: A survey," *ACM Computing Surveys*, vol. 52, no. 3, pp. 1–36, May 2019, doi: 10.1145/3310194.
[9]   A. Khalili, A. Soliman, M. Asaduzzaman, and A. Griffiths, "Wi-Fi sensing: applications and challenges," *The Journal of Engineering*, vol. 2020, no. 3, pp. 87–97, Mar. 2020, doi: 10.1049/joe.2019.0790.
[10]   B. Yang, L. Guo, R. Guo, M. Zhao, and T. Zhao, "A novel trilateration algorithm for RSSI-based indoor localization," *IEEE Sensors Journal*, vol. 20, no. 14, pp. 8164–8172, Jul. 2020, doi: 10.1109/JSEN.2020.2980966.
[11]   J. Wang and J. G. Park, "An enhanced indoor positioning algorithm based on fingerprint using fine-grained CSI and RSSI measurements of IEEE 802.11n WLAN," *Sensors*, vol. 21, no. 8, p. 2769, Apr. 2021, doi: 10.3390/s21082769.
[12]   J. Liu, H. Liu, Y. Chen, Y. Wang, and C. Wang, "Wireless sensing for human activity: a survey," *IEEE Communications Surveys and Tutorials*, vol. 22, no. 3, pp. 1629–1645, 2020, doi: 10.1109/COMST.2019.2934489.
[13]   A. Rafay, S. M. Idrus, K. M. Yusof, and S. H. Mohammad, "A survey on advanced transmission technologies for high bandwidth and good signal quality for high-speed railways," *Indonesian Journal of Electrical Engineering and Computer Science*, vol. 23, no. 1, pp. 293–301, Jul. 2021, doi: 10.11591/ijeecs.v23.i1.pp293-301.
[14]   A. M. Jaradat, J. M. Hamamreh, and H. Arslan, "Modulation options for OFDM-based waveforms: classification, comparison, and future directions," *IEEE Access*, vol. 7, pp. 17263–17278, 2019, doi: 10.1109/ACCESS.2019.2895958.
[15]   S. Tan, J. Yang, and Y. Chen, "Enabling fine-grained finger gesture recognition on commodity WiFi devices," *IEEE Transactions on Mobile Computing*, vol. 21, no. 8, pp. 2789–2802, Aug. 2022, doi: 10.1109/TMC.2020.3045635.
[16]   W. Liu *et al.*, "Survey on CSI-based indoor positioning systems and recent advances," in *2019 International Conference on Indoor Positioning and Indoor Navigation, IPIN 2019*, Sep. 2019, pp. 1–8, doi: 10.1109/IPIN.2019.8911774.
[17]   Y. He, Y. Chen, Y. Hu, and B. Zeng, "WiFi vision: sensing, recognition, and detection with commodity MIMO-OFDM WiFi," *IEEE Internet of Things Journal*, vol. 7, no. 9, pp. 8296–8317, Sep. 2020, doi: 10.1109/JIOT.2020.2989426.
[18]   H. Li, X. He, X. Chen, Y. Fang, and Q. Fang, "Wi-motion: A robust human activity recognition using WiFi signals," *IEEE Access*, vol. 7, pp. 153287–153299, 2019, doi: 10.1109/ACCESS.2019.2948102.
[19]   M. A. A. Al-Qaness *et al.*, "Channel state information from pure communication to sense and track human motion: A survey," *Sensors (Switzerland)*, vol. 19, no. 15, p. 3329, Jul. 2019, doi: 10.3390/s19153329.
[20]   J. Wang and J. G. Park, "A novel indoor ranging algorithm based on a received signal strength indicator and channel state information using an extended kalman filter," *Applied Sciences (Switzerland)*, vol. 10, no. 11, p. 3687, May 2020, doi: 10.3390/app10113687.
[21]   D. Halperin, W. Hu, A. Sheth, and D. Wetherall, "Tool release: Gathering 802.11n traces with channel state information," *Computer Communication Review*, vol. 41, no. 1, p. 53, Jan. 2011, doi: 10.1145/1925861.1925870.
[22]   X. Li, X. Cai, Y. Hei, and R. Yuan, "NLOS identification and mitigation based on channel state information for indoor WiFi localisation," *IET Communications*, vol. 11, no. 4, pp. 531–537, Mar. 2017, doi: 10.1049/iet-com.2016.0562.
[23]   G. Forbes, "Gi-z/CSIKit: Python CSI processing and visualisation tools for Atheros, Intel, Nexmon, ESP32, and PicoScenes (USRP, etc) formats.," Github, 2023. Accessed: Mar. 17, 2023. [Online]. Available: https://github.com/Gi-z/CSIKit.
[24]   A. Zhuravchak, O. Kapshii, and E. Pournaras, "Human activity recognition based on Wi-Fi CSI data - a deep neural network approach," *Procedia Computer Science*, vol. 198, pp. 59–66, 2021, doi: 10.1016/j.procs.2021.12.211.
[25]   "CSI-tool-camera-shooting/csi_fun.h at master qiyinghua/CSI-Tool-Camera-Shooting," Github, 2023. Accessed: Mar. 17, 2023. [Online]. Available: https://github.com/qiyinghua/CSI-Tool-Camera-Shooting.

BIOGRAPHIES OF AUTHORS

Hicham Boudlal [ID] [⚏] [SC] [◔] has obtained his engineering degree in networks and telecommunications from ENSA Oujda in 2017. In 2021, he joined the ACSA Laboratory at the Faculty of Sciences, Mohammed First University, Oujda, Morocco. His main research interests include network architecture, network security, channel state information, and WiFi sensing. He can be contacted at email: hicham.boudlal5@gmail.com.

Mohammed Serrhini is professor with the Department of Computer Science at Faculty of Sciences, Mohamed First University, Oujda, Morocco. His research interests are in the areas of computer vision, image processing, brain computer interface in education, and security. He can be contacted at email: serrhini@gmail.com.

Ahmed Tahiri received Ph.D. in numerical analysis at the free University of Brussels (ULB). He is a professor at the Department of Computer Science, Faculty of Sciences at the University Mohammed First, Morocco. His research interests include issues related to numerical approximations and their optimal implementations. Recently, he is interested in intelligent systems. He can be contacted at email: tahiriahmed02@yahoo.fr.